

Article

# A New Feature Extraction Method Based on EEMD and Multi-Scale Fuzzy Entropy for Motor Bearing

Huimin Zhao <sup>1,2,3,4,5</sup>, Meng Sun <sup>1</sup>, Wu Deng <sup>1,2,3,4,5,\*</sup> and Xinhua Yang <sup>1</sup>

<sup>1</sup> Software Institute, Dalian Jiaotong University, Dalian 116028, China; hm\_zhao1977@126.com (H.Z.); lunwen1209@yeah.net (M.S.); yangxh@djtu.edu.cn (X.Y.)

<sup>2</sup> Sichuan Provincial Key Lab of Process Equipment and Control, Sichuan University of Science and Engineering, Zigong 64300, China

<sup>3</sup> Traction Power State Key Laboratory, Southwest Jiaotong University, Chengdu 610031, China

<sup>4</sup> The State Key Laboratory of Mechanical Transmissions, Chongqing University, Chongqing 400044, China

<sup>5</sup> Dalian Key Laboratory of Welded Structures and Its Intelligent Manufacturing Technology (IMT) of Rail Transportation Equipment, Dalian Jiaotong University, Dalian 116028, China

\* Correspondence: dw7689@163.com; Tel.: +86-411-8410-5386

Academic Editors: Carlo Cattani and Kevin H. Knuth

Received: 23 September 2016; Accepted: 26 December 2016; Published: 31 December 2016

**Abstract:** Feature extraction is one of the most important, pivotal, and difficult problems in mechanical fault diagnosis, which directly relates to the accuracy of fault diagnosis and the reliability of early fault prediction. Therefore, a new fault feature extraction method, called the EDOMFE method based on integrating ensemble empirical mode decomposition (EEMD), mode selection, and multi-scale fuzzy entropy is proposed to accurately diagnose fault in this paper. The EEMD method is used to decompose the vibration signal into a series of intrinsic mode functions (IMFs) with a different physical significance. The correlation coefficient analysis method is used to calculate and determine three improved IMFs, which are close to the original signal. The multi-scale fuzzy entropy with the ability of effective distinguishing the complexity of different signals is used to calculate the entropy values of the selected three IMFs in order to form a feature vector with the complexity measure, which is regarded as the inputs of the support vector machine (SVM) model for training and constructing a SVM classifier (EOMSMFD based on EDOMFE and SVM) for fulfilling fault pattern recognition. Finally, the effectiveness of the proposed method is validated by real bearing vibration signals of the motor with different loads and fault severities. The experiment results show that the proposed EDOMFE method can effectively extract fault features from the vibration signal and that the proposed EOMSMFD method can accurately diagnose the fault types and fault severities for the inner race fault, the outer race fault, and rolling element fault of the motor bearing. Therefore, the proposed method provides a new fault diagnosis technology for rotating machinery.

**Keywords:** feature extraction; motor bearing; ensemble empirical mode decomposition (EEMD); multi-scale fuzzy entropy; correlation coefficient method; SVM; fault diagnosis

## 1. Introduction

Rolling bearing is one of the most important parts of rotating machinery. Its operation state directly determines whether the whole machine is safe, efficient, and reliable. However, due to the influences of transferring load and the additional load by the gear meshing in motor bearing, the fault rate of rolling bearing is always high without decreasing, and even shows an upward trend sometimes. Therefore, it is becoming increasingly important to improve the reliability of rolling bearings and to accurately detect bearing faults in time. When motor bearing faults occur, the periodic pulse impact force is generated, the nonlinear vibration of the mechanical system causes a collected vibration signal

that often takes on nonlinear and non-stationary characteristics. At the same time, the fault will rapidly develop and the collected vibration signals often contain a large amount of noise. Moreover, the early fault features of the bearing in the vibration signal is relatively weak, which easily overwhelms the signal due to the noise. It is generally known that the bearing is one of the most vulnerable components in the motor and is where faults occur. Bearing damage constitutes about 44% of the total number of motor faults [1]. Therefore, accurately extracting fault features from the motor bearing and successfully separating the fault mode has been a serious and difficult problem.

In order to effectively extract fault features of bearing from the vibration signal, many scholars have proposed many effective methods, such as short time Fourier transform (STFT), wavelet transform (WT), Hilbert–Huang transform (HHT), empirical mode decomposition (EMD), ensemble empirical mode decomposition (EEMD), entropy, and so on [2–5]. Seker and Ayaz [6] proposed a new method to extract features from the measured vibration signals in motors subjected to accelerated bearing fluting aging and to detect the effects of bearing fluting at each aging cycle of induction motors. Yang et al. [7] proposed a fault diagnosis method based on empirical mode decomposition energy entropy according to the non-stationary characteristics of roller bearing fault vibration signals. Cheng et al. [8] proposed a new fault feature extraction approach based on EMD method and an autoregressive model for roller bearings. Cheng et al. [9] proposed a local rub-impact fault diagnosis method of a rotor system based on empirical mode decomposition. Immovilli et al. [10] compared the bearing fault detection capability obtained with the vibration and current signals. These studies contributed to the use of a simple and effective signal processing technique for both current and vibration signals. Lei et al. [11] proposed an automated and effective fault diagnosis method of a locomotive roller bearing based on ensemble empirical mode decomposition and a wavelet neural network. Wang et al. [12] proposed a bearing fault diagnosis method (named cyclic spike detection method) to extract weak bearing fault features from a multi-component signal mixture. Liu et al. [13] proposed frequency band entropy based on short-time Fourier transform to detect hidden periodical components in signals and extract fault features from strong background noises. Wang et al. [14] proposed a new method for diagnosing faults and assessing the health of bearings by using the Mahalanobis–Taguchi system. Liao and Li [15] proposed a hybrid fault-feature extraction method by detecting localized defects and analyzing vibration signals of rolling element bearings via customized multi-wavelet packet transform and a swarm fish algorithm. Wang et al. [16] proposed an early weak fault feature extraction method of a rolling bearing based on ensemble empirical mode decomposition and tunable Q-factor wavelet transform. Ahn et al. [17] proposed a fault detection method of a roller bearing system by using a wavelet denoising scheme and a proper orthogonal value of an intrinsic mode function covariance matrix. Jiang et al. [18] proposed a novel approach of condition monitoring and fault diagnosis for rolling element bearings based on an improved ensemble empirical mode decomposition. Zhu et al. [19] proposed a roller bearing fault diagnosis method based on hierarchical entropy and a support vector machine with a particle swarm optimization algorithm. Gao et al. [20] proposed a novel time–frequency distribution matrix factorization method based on combining the concepts of a time–frequency distribution with non-negative matrix factorization to enhance representation and identification of bearing faults. Henao et al. [21] reviewed the trends of diagnostic techniques in fault diagnoses for electrical machines in recent years. The total number of operating electrical machines in the world was around 16.1 billion in 2011. Lucia et al. [22] proposed a novel technique based on the stray flux measurement in different positions around the electrical machine, and reports an extensive survey on the stray-flux-based fault detection methods for induction motors. Wang et al. [23] proposed a general sequential Monte Carlo method and a joint posterior probability density function of wavelet parameters by a set of random particles with their associated weights for extracting bearing fault features. He et al. [24] proposed an ensemble super-wavelet transform based on the combination of tunable Q-factor wavelet transform and Hilbert transform for investigating the vibration features of induction motor bearing faults. Wang et al. [25] proposed an early weak fault diagnosis method of rolling bearing based on minimum entropy de-convolution and a fast Kurtogram algorithm.

Wang et al. [26] proposed a novel non-negative empirical mode decomposition manifold method for feature extraction from the fault-related intrinsic mode functions in machinery fault diagnosis. Shi et al. [27] proposed a method of empirical mode decomposition based on a cascaded multi-stable stochastic resonance system. Wang et al. [28] proposed a novel faint signal extraction method by a time–frequency distribution image dimensionality reduction in order to overcome the shortcomings of the fast Kurtogram method. Li et al. [29] proposed a new bearing vibration feature extraction method based on self-adaptive time–frequency analysis, multi-scale permutation entropy, and an improved support vector machine based on a binary tree for rolling bearings.

In recent years, many feature extraction methods based on nonlinear dynamics parameters have been proposed, such as fractal dimension, approximate entropy, sample entropy, and so on. They are widely used in signal analysis and processing of machinery and have become new methods for analyzing nonlinear time series. Approximate entropy was proposed by Pincus and applied to analyze physiological time series [30]. However, the approximate entropy has its matching features [31]. Richman et al. [32] proposed sample entropy for compensating approximate entropy defects. Approximate entropy and sample entropy are statistical indexes for measuring the complexity of the signal. When two models are evaluated to be similar or not, the given threshold is used as the criterion. If the distance between two models shows small changes near the threshold parameter, it will cause different discriminated results and affect statistical stability. For this problem, Chen [33,34] proposed the fuzzy entropy method. This method used the membership function instead of the hard threshold criterion in fuzzy theory. Fuzzy entropy is used to measure physiological signals and obtain an improved measure effect. On the basis of studies, some new entropy methods are proposed for feature extraction, such as scale entropy [35], multi-scale entropy [36,37], multi-scale permutation entropy [38–40], and multi-scale fuzzy entropy [41]. For the vibration signals of mechanical equipment, the vibration signals of different faults have different complexities, and the probability of generating new models are different. Thus, the entropy values are also different. Moreover, some faults usually appear in a certain frequency band. The fault types are different, as are the corresponding characteristic frequency bands. The signal in the fault frequency band changes, and its complexity will change. Thus, the values of multi-scale fuzzy entropy are used as the fault feature index for the pattern recognition of rolling bearing faults in this paper.

These proposed methods have their own limitations in feature extraction and fault diagnosis for rotating machinery. In a mechanical fault diagnosis, wavelet transform has achieved good results, but it is not clear as to how wavelet function can be chosen with improved time and frequency resolution. The threshold of manual operation needs to be determined. The EMD method has been widely used, but there are problems of mode mixing, end effects, over envelope, under envelope, and so on in the decomposition signal. The EEMD method is an improved EMD method, which can adaptively decompose the signal into a series of IMFs with different time scales according to the characteristics of the signal, and can effectively solve existing problems. Multi-scale fuzzy entropy measures the complexity of the time series under different scales and the probability of generating new information under a new dimension. It is a new method based on multi-scale entropy and fuzzy entropy and takes on the advantages of small data, anti-noise, and relative consistency.

Due to the complexity of the mechanical system, the vibration signal contains related fault information, which is often distributed at different scales. The different fault vibration signals have different complexities, the probability of the generated new model is also different, and the entropy is also different. Thus, the multi-scale analysis method is a valid method for calculating the entropy values to generate the fault feature vector. When the bearing fault occurs, the complexity of the vibration signal will change. For different fault types and severities, the frequencies of the friction and impact are different. The complexities of the corresponding vibration signals are also different. Thus, a new fault feature extraction of the motor bearing based on EEMD, mode selection, and multi-scale fuzzy entropy is proposed in this paper. The EEMD is used to decompose the vibration signal into a series of IMFs with specific physical meanings. Then, three more sensitive IMFs are selected to represent the

original signal by using the correlation coefficient method. Moreover, the multi-scale fuzzy entropy is used to extract the features of different faults under different scales. The support vector machine (SVM) classifier is used to classify, identify, and determine the working condition and fault type of the motor bearing. The effectiveness of the proposed method is verified by analyzing and testing the fault signal of a real motor bearing.

## 2. EEMD, Multi-Scale Fuzzy Entropy, and SVM

### 2.1. EEMD

The empirical mode decomposition (EMD) is an adaptive decomposition technique [8]. It is based on the direct extraction of the energy associated with various intrinsic time scales in order to generate a collection of IMFs. The EMD method can decompose the complicated signal into a definite number of high-frequency and low-frequency components by means of a process called “sifting”. However, the reasonable IMFs depend on the existence of the extreme points of the signal and the distribution of the extreme points in the EMD method. The discontinuity of IMFs will result in the generation of mode mixing. Ensemble empirical mode decomposition (EEMD) [16] method is an improvement of the EMD method, which can solve the problem of mode mixing in the process of EMD decomposition by adding the Gauss white noise. It defines the true IMF components as the mean of an ensemble of trials. Each trial consists of the decomposition results of the signal plus with a white noise of finite amplitude. Thus, the EEMD significantly reduces the mode mixing of EMD. The principle of the EEMD method is described as follows. The added white noise uniformly fills the whole time–frequency space, promotes the natural separation of frequency scales, and reduces the occurrence of mode mixing by the discontinuity of IMFs in the EMD method. The EEMD method can be described as follows:

- Step 1: Initialize the EMD method. The total operation number is  $M$ , the amplitude coefficient of added white noise is  $k$ , and the execution number is  $m = 1$ .
- Step 2: The numerically generated white noise  $x_m(t)$  with the given amplitude to the original signal  $x(t)$  is generated:

$$x_m(t) = x(t) + k * N_m(t) \quad (1)$$

where  $x(t)$  is the original signal,  $k$  is the amplitude coefficient, and  $N_m(t)$  is meant to randomly add the white noise.

- Step 3: The EMD method is used to decompose  $x_m(t)$  into a series of IMF components  $C_{j,m}$ .  $C_{j,m}$  is the  $j$ -th IMF of the  $m$ -th decomposition:

$$x_m(t) = \sum_{j=1}^S C_{j,m}(t) + r_{j,m}(t)$$

where  $S$  is the number of IMFs,  $r_{j,m}(t)$  is the final residue, which is the mean trend of the signal, and  $C_{j,m}(t)$  represents the IMFs, which include different frequency bands ranging from the high frequency to low frequency.

- Step 4: If the decomposition number is  $m < M$ , then  $m = m + 1$ . Then, return to Step 2.
- Step 5: The average of the corresponding is calculated for the  $M$ -th decomposition. The calculation result is obtained:

$$\bar{C}_j(t) = \frac{1}{M} \sum_{i=1}^M C_{j,m}(t) \quad (2)$$

where  $\bar{C}_j(t)$  is the  $j$ -th IMF decomposed by EEMD when  $m = 1, 2, 3, \dots, M$  and  $j = 1, 2, 3, \dots, S$ .

In the EEMD method, the total operation number  $M$  and the noise amplitude  $\alpha$  are the two parameters that need to be given. Then, the added white noise series cancel each other in the final average value of the corresponding IMFs in order to increase the signal-to-noise ratio. Thus, the two

parameters should be selected carefully. It should be noted that the number of ensemble numbers should increase when the amplitude of noise increases so as to reduce the contribution of added noise in the decomposed results.

### 2.2. Fuzzy Entropy

Entropy is a general concept, which is used to measure the uncertainty of a piece of information. The fuzzy degree is a quantitative index to describe the degree of fuzzy data. Fuzzy entropy is a technique to measure the complexity of time series based on the concept of approximate entropy and sample entropy. The fuzzy entropy is described as follows:

(1) Give an  $N$  sample time series  $\{u(i) : 1 \leq i \leq N\}$ . For a given  $m, n$ , and  $r$ , a vector set  $\{X_i^m, i = 1, 2, \dots, N - m + 1\}$  is formed. Each vector contains  $m$  sequential elements from  $u(i)$  as follows:

$$X_i^m = \{u(i), u(i + 1), \dots, u(i + m - 1)\} - u_0(i) \tag{3}$$

where  $u_0(i)$  is the average of vector  $X_i^m$ :

$$u_0(i) = \frac{1}{m} \sum_{j=0}^{m-1} u(i + j). \tag{4}$$

(2) For a certain vector  $X_i^m$ , define the distance  $d_{ij}^m$  between  $X_i^m$  and  $X_j^m$  ( $j = 1, 2, 3, \dots, N - m, i \neq j$ ) as the maximum difference of the corresponding scalar components:

$$d_{ij}^m = d[X_i^m, X_j^m] = \max_{k \in (0, m-1)} [(u(i + k) - u_0(i)) - (u(j + k) - u_0(j))]. \tag{5}$$

(3) Give  $n$  and  $r$ , and calculate the similarity degree  $D_{ij}^m$  of  $X_j^m$  to  $X_i^m$  through a fuzzy function  $\mu(d_{ij}^m, n, r)$ :

$$D_{ij}^m(n, r) = \mu(d_{ij}^m, n, r) = e^{-\ln 2(d_{ij}^m/r)^n} b. \tag{6}$$

(4) Define the function  $\varphi^m$  as follows:

$$\varphi^m(n, r) = \frac{1}{N - m} \sum_{i=1}^{N-m} \left( \frac{1}{N - m + 1} \sum_{j=1, j \neq i}^{N-m} D_{ij}^m \right). \tag{7}$$

(5) Similarly, form  $\{X_i^{m+1}\}$  and obtain the function  $\varphi^{m+1}$ .

$$\varphi^{m+1}(n, r) = \frac{1}{N - m} \sum_{i=1}^{N-m} \left( \frac{1}{N - m + 1} \sum_{j=1, j \neq i}^{N-m} D_{ij}^{m+1} \right). \tag{8}$$

(6) Fuzzy entropy of sequence  $\{u(i) : 1 \leq i \leq N\}$  as the negative natural logarithm of the deviation of from is defined as follows:

$$FuzzyEn(m, n, r) = \lim_{N \rightarrow \infty} [\ln \varphi^m(n, r) - \ln \varphi^{m+1}(n, r)]. \tag{9}$$

(7) If the length  $N$  is finite,  $FuzzyEn(m, n, r)$  can be changed as follows:

$$FuzzyEn(m, n, r) = \ln \varphi^m(n, r) - \ln \varphi^{m+1}(n, r). \tag{10}$$

### 2.3. Multi-Scale Entropy

Because the sample entropy is used to measure the complexity of the time series in one scale. Costa et al. [42] proposed the concept of multi-scale entropy in 2002, which is used to measure the

complexity and self-similarity of time series under different scale factors. The multi-scale entropy is defined as the sample entropy of time series under different scales. This takes on the characteristics of fast computation and anti-interference under multi-scale factors. If one sequence of entropy values is larger than the other sequence of entropy values under more scales, the sequence is more complex than the other sequence. If one sequence of entropy values monotonically decreases with increasing scale factors, then the sequence structure is relatively simple. It contains more information in the smallest scales. If one sequence of entropy values monotonically increases with increasing scale factors, then the sequence contains more information in the multiple scales.

The multi-scale entropy is described as follows:

(1) The time series  $\{u(i) : 1 \leq i \leq N\}$  with length of  $N$  is processed by the multi-scale:

$$y_j^\tau = \frac{1}{\tau} \sum_{i=(j-1)\tau+1}^{j\tau} u(i), \quad 1 \leq j \leq \frac{N}{\tau} \quad (11)$$

where  $y_j^\tau$  is the time series of coarse-grained procedure.  $\tau = 1, 2, \dots$  is the scale factor, which divides the original sequence  $u(i)$  into  $\tau$  segments.

(2) Construct a vector with  $m$  dimensions:

$$x_m(i) = \{y_{i+k} : 0 \leq k \leq m-1\}. \quad (12)$$

(3) Calculate the distance  $d[x_m(i), x_m(j)]$  between  $x_m(i)$  and  $x_m(j)$ .

(4) Set the similarity tolerance value  $r (r > 0)$ . For each  $i$ , the total number  $B_m(i)$  ( $d < r$ ) is counted, and the ratio is also calculated:

$$C_r^m(i) = \frac{B_m(i)}{M-m}. \quad (13)$$

(5) Calculate the average value  $C^m(r)$  of  $C_r^m(i)$ .

(6) Add dimension to  $m+1$ , and repeat (2) to (5). Calculate the  $C^{m+1}(r)$  and  $C_r^{m+1}(r)$ . When the length of the sequence is  $N$ , the estimated value of sample entropy is described as follows:

$$PE_{IMF_k}(m, r, N). \quad (14)$$

(7) In one scale factor, the sample entropy value is used to form the multi-scale entropy feature vector:

$$S = \{PE_{IMF_1}, PE_{IMF_2}, \dots, PE_{IMF_k}\}. \quad (15)$$

#### 2.4. Multi-Scale Fuzzy Entropy

The multi-scale analysis algorithm was developed to quantify the complexity of the time series in the real world. On the basis of the concept of multi-scale analysis, Zheng et al. [41] proposed multi-scale fuzzy entropy (MFE) for rolling bearing fault diagnosis. The MFE technology contains two steps. Firstly, the coarse-grained procedure is used to obtain a time series with multiple scales from the original time series. Secondly, the fuzzy entropy at each coarse-grained time series is calculated. Two procedures of MFE technology are described as follows:

(1) Obtain the coarse-grained time series at a scale factor of  $\tau$  ( $\tau$  is a positive integer). The original time series are divided into disjointed windows with length  $\tau$ , and the data points are averaged inside each window. Namely, the coarse-grained time series at a scale factor of  $\tau$ ,  $y_\tau$  can be constructed according to the expression.

$$y_j^\tau = \frac{1}{\tau} \sum_{i=(j-1)\tau+1}^{j\tau} u(i), \quad 1 \leq j \leq \frac{N}{\tau}. \quad (16)$$

(2) In MFE technology, the fuzzy entropy of each coarse-grained time series is calculated and then plotted as the function of the scale factor,  $\tau$ , which can be expressed as

$$MFE(x, \tau, m, r) = \text{FuzzyEn}(y_j^{\tau, m, r}). \quad (17)$$

Note that the  $r$  in the calculation for different scales is same, which is obtained by the  $r = \lambda \times SD$  and  $SD$  is the standard deviation of the original time series.

## 2.5. SVM

The support vector machine (SVM), introduced by Vapnik, is one of the most popular tools in bioinformatics for a supervised machine learning methods based on structural risk minimization [43–47]. The basic characteristic of SVM is to map the original nonlinear data into a higher dimensional feature space, where a hyperplane is constructed to bisect two classes of data and maximize the margin of separation between itself and those points lying nearest to it (the support vectors). The hyperplane should be used as the basis for classifying unknown data. Thus, the SVM was widely applied in pattern recognition, nonlinear system identification, modeling, predication, control, and so on. The SVM is mainly used to solve the binary classification problem. The theory was originally derived from data classification. The purpose of the SVM is to find one division plane meeting the given requirement in order to keep the point of the training set far away the plane. In other words, it is to find one split plane to keep the largest classification interval (margin). The SVM originated from the optimal classification surface from the linearly separable circumstance. It is used to solve the linear constraint quadratic programming problem by mapping the input space into the high dimensional inner product space to obtain the global optimal solution to guarantee convergence speed and avoid the local minimum.

## 3. Fault Diagnosis Method

The key to fault diagnosis is choosing the appropriate method to identify the type, quantity, location, and severity of fault based on the fault mechanism [48,49]. Extracting mechanical fault feature information from the fault vibration signal using a suitable signal analysis method is one of the most important steps. The EEMD method is an improved EMD method, which can effectively avoid mode mixing in the process of EMD decomposition by adding Gaussian white noise. It uses the statistical properties of Gaussian white noise to decompose the vibration signal in order to obtain an uniform distribution of frequency. Multi-scale fuzzy entropy based on multi-scale analysis and fuzzy entropy can effectively obtain multiple scale time series from the original time series and calculate the fuzzy entropy value of each coarse-grained time series. The SVM based on structural risk minimization is one of the most popular tools. It can map the original nonlinear data into a higher-dimensional feature space. Thus, in order to effectively extract fault feature information and diagnose the faults from the vibration signal, the advantages of each method are fully utilized, and a new fault diagnosis (EOMSMFD) method based on combining EEMD, model selection, multi-scale fuzzy entropy and SVM is proposed to realize fault diagnosis. In the proposed EOMSMFD method, fault vibration signals of the inner ring, the outer ring, and the rolling element of the motor bearing are decomposed into a series of IMFs and residual components by using the EEMD method with appropriate parameters. Then, the correlation coefficient between each component and original signal are calculated in the frequency domain. The value of the correlation coefficient is between 0 and 1. The component correlation with a larger value shows that the component is more related to the original signal. Three components with larger value of correlation coefficient are selected here. Next, the parameters of multi-scale fuzzy entropy are selected according to the characteristics of signal, and the values of multi-scale fuzzy entropy of three selected components are calculated to form a feature vector with the complexity measure. The obtained entropy values are selected as characteristic vectors to train the SVM model and

construct a SVM classifier for fulfilling fault pattern recognition. The flow of the proposed EOMSMFD method is shown in Figure 1.

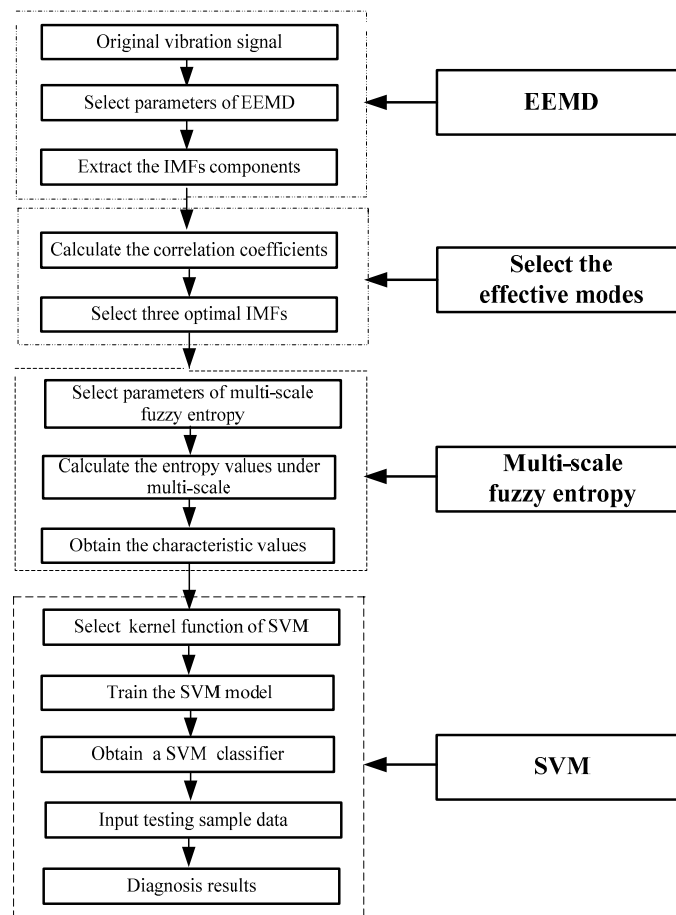


**Figure 1.** The flow of the EOMSMFD method.

#### 4. Fault Feature Extraction of the Bearing Fault of AC Motor

##### 4.1. Experimental Environment and Data

In order to validate the effectiveness of the proposed feature extraction method, the vibration data are used from the Bearing Data Center of Case Western Reserve University [50]. The 6205-2RS 6 JEM SKF deep groove ball bearing is employed in the experiment. The motor with 1.5 KW is connected to a dynamometer and torque sensor by a self-aligning coupling. The data were collected from an accelerometer mounted on the radial vertical direction of the motor. The used vibration data were measured under no-load (0 HP) and load (3 HP) at rotation speeds (1797 r/min and 1730 r/min). Faults were introduced to the bearings using the electro-discharge machining method. The fault diameters were 0.007 and 0.021 in., which are used in the experiment. The three different faults are: (1) the inner race fault; (2) the outer race fault; (3) the rolling element. The bearing vibration data was sampled at a frequency of 12,000 Hz, and the duration of each vibration signal was 10 s.

The motor bearing with no-load and a fault diameter of 0.007 in. is selected here, which is used to show the time-domain waveform of the fault vibration signal. The time-domain waveforms of the original vibration signals are shown in Figures 2–4. Figure 2 is the time-domain waveform of the fault vibration signal of the inner race. Figure 3 is the time-domain waveform of the fault vibration signal of the outer race. Figure 4 is the time-domain waveform of the fault vibration signal of the rolling element.



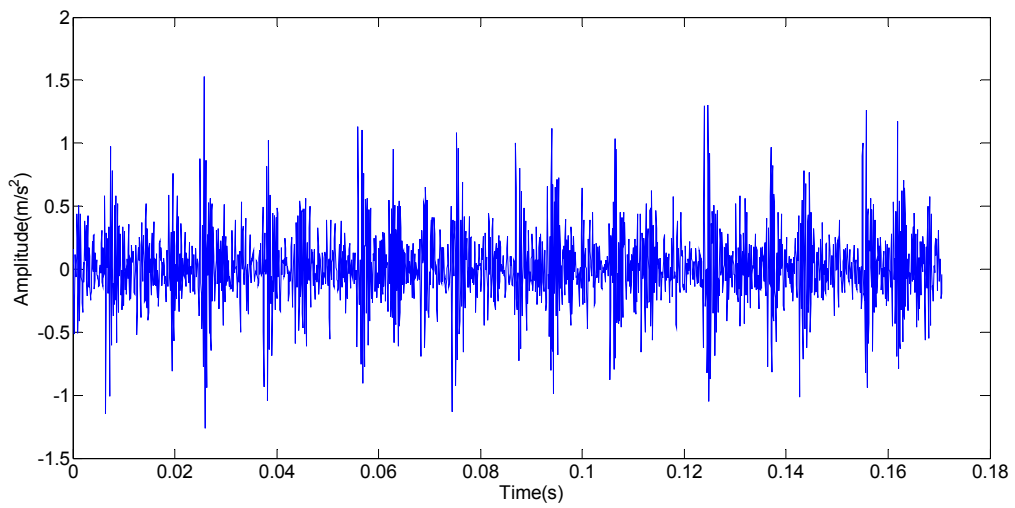


**Figure 2.** The time-domain waveform of the inner race fault signal.

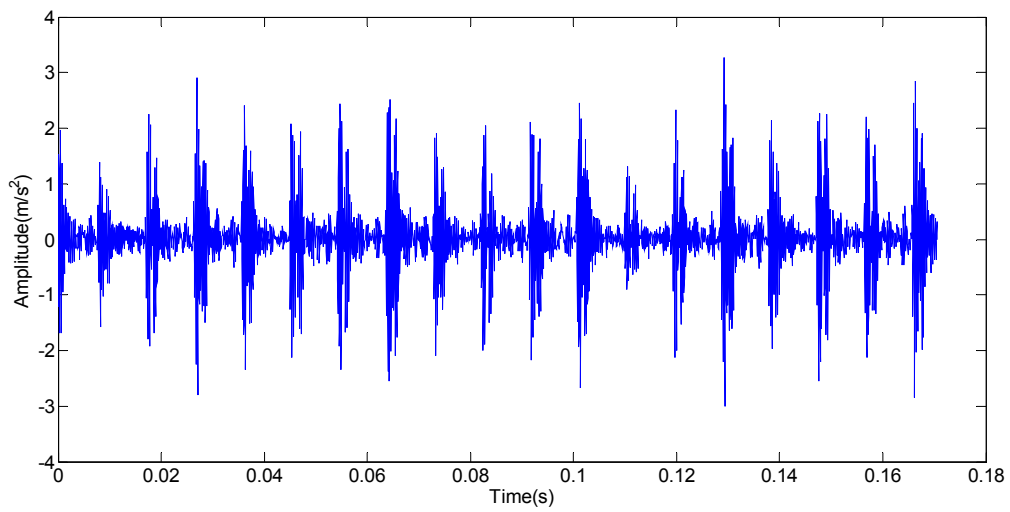


**Figure 3.** The time-domain waveform of the outer race fault signal.

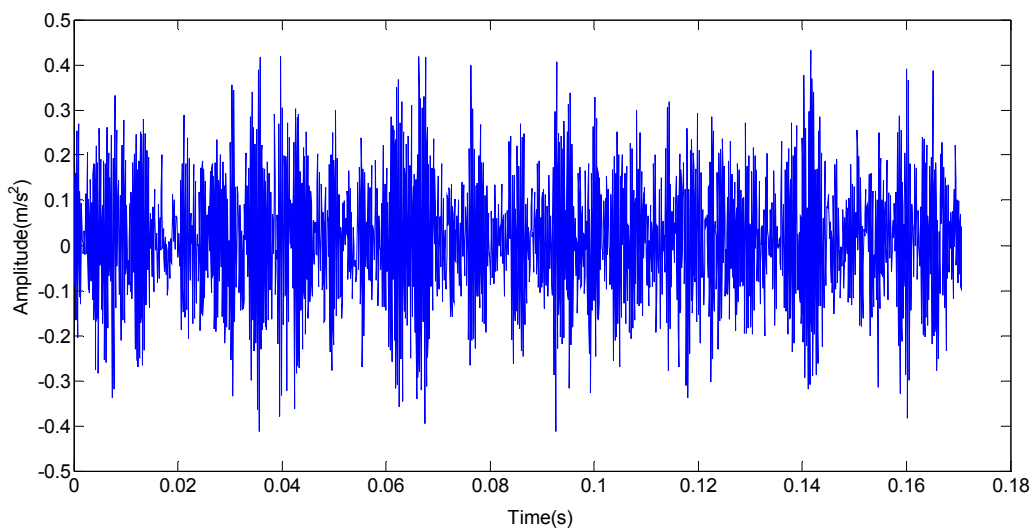


**Figure 4.** The time-domain waveform of the rolling element fault signal.

#### 4.2. Vibration Signal Decomposition Based on the EEMD Method

As can be seen from the definition of the EEMD method and the signal decomposition process, the decomposition results by the EEMD method are not only related to the signal itself, but are also related to the standard deviation of added white noise with a noise level and a maximum number of iterations. In order to consider the comprehensive performance, the standard deviation of random white noise is  $Nstd = 0.2$ , the white noise level is  $SNR = 500$ , and the maximum number of iterations is  $MaxIter = 5000$  here. The motor bearing with no-load and a fault diameter of 0.007 in. is selected. The EEMD decomposition results for three fault conditions are shown in Figures 5–7.

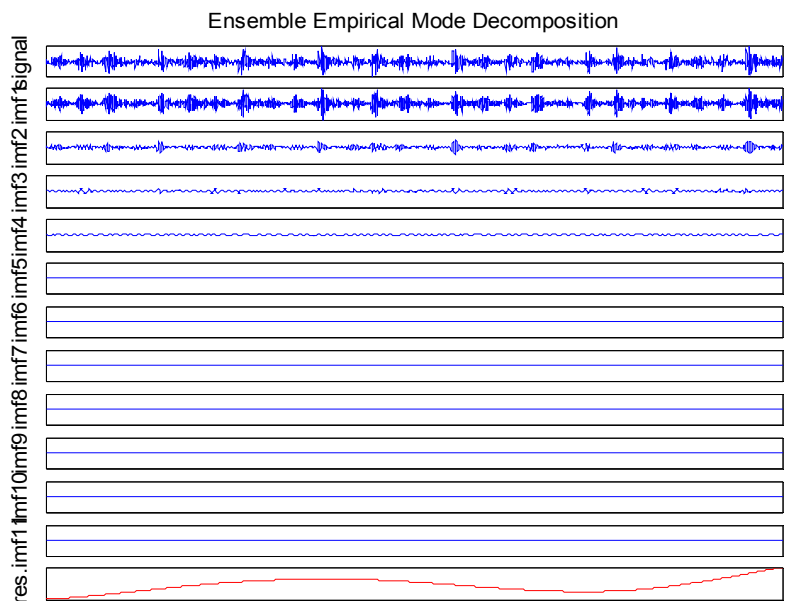


Figure 5. Decomposition result of the inner race fault by the EEMD method.

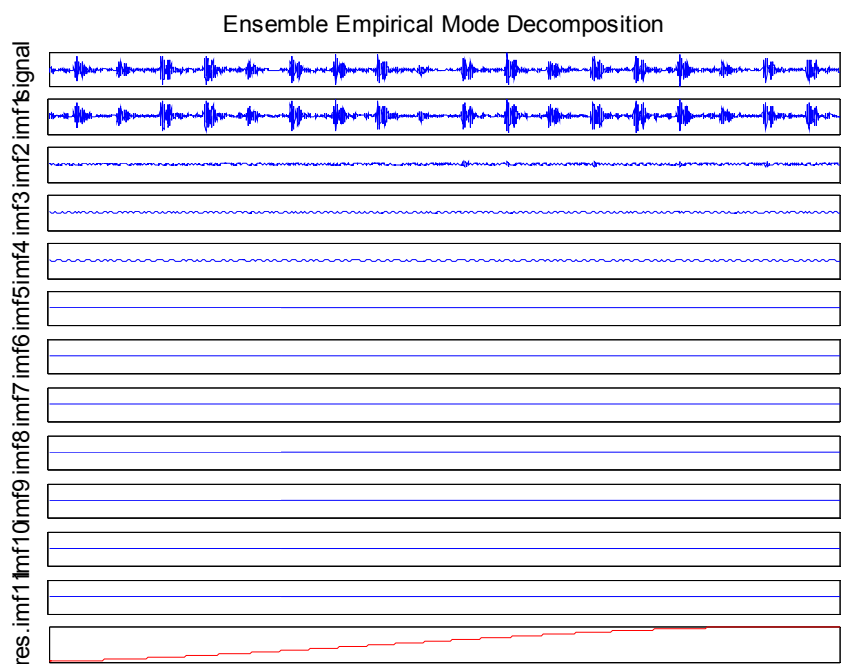


Figure 6. Decomposition result of the outer race fault by the EEMD method.

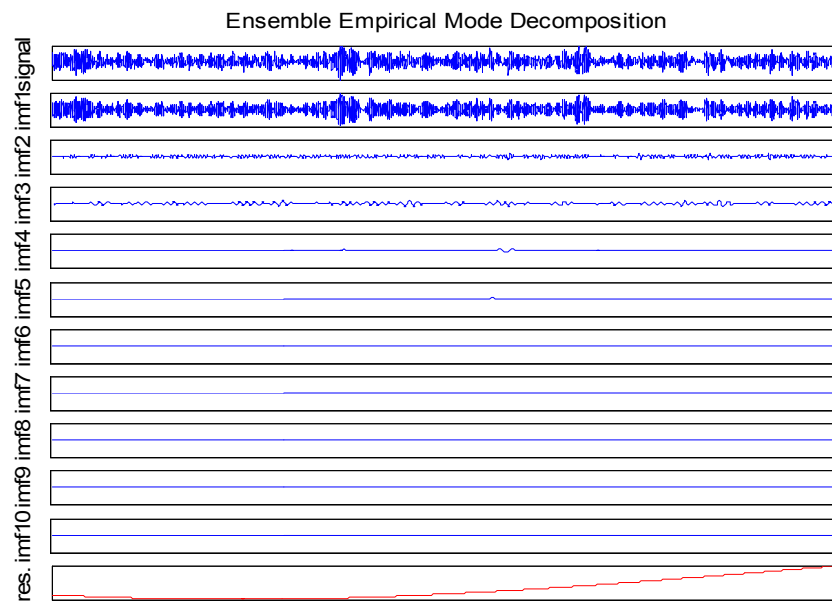


Figure 7. Decomposition result of the rolling element fault by the EEMD method.

#### 4.3. Selection of Major Modes

Three IMF components with a larger value of correlation coefficient are selected after the signals are decomposed by using the EEMD method. Compared with the time domain analysis, frequency domain analysis is more concise, profound, and convenient. Therefore, the frequency domain correlation coefficient method is used to measure the correlation between each component and the original signal after the signals are decomposed by using the EEMD method. The frequency domain correlation coefficient  $\rho_{x,c_i}$  can be expressed by the following equation:

$$\rho_{x,c_i} = \left| \frac{E[(c_i(f) - u_{c_i})(X(f) - u_x)]}{\sigma_{c_i}\sigma_x} \right| \quad (18)$$

where  $X(f)$  represents the frequency components of the original signal  $X(t)$ , and  $C_i(f)$  represents the frequency components of  $\bar{C}_i$  in Equation (2).  $u_{c_i}$ ,  $u_x$ ,  $\sigma_{c_i}$ , and  $\sigma_x$  are the corresponding frequency domain mean and deviation of  $C_i(f)$  and  $X(f)$ , respectively.

The frequency correlation coefficient  $\rho_{x,c_i}$  reflects the correlation between the IMF components and the original signal in the frequency domain. The correlation coefficient  $\rho_{x,c_i}$  is between 0 and 1. When  $\rho_{x,c_i}$  is equal to 0, it shows that the IMF component is completely uncorrelated to the original signal. When  $\rho_{x,c_i}$  is equal to 1, it shows that the IMF component is completely correlated to the original signal. If the value of  $\rho_{x,c_i}$  is larger, it shows that the  $f_k(t)$  component is more related to the original signal. Thus, the IMF components are rearranged from a high value to a low value according to the  $\rho_{x,c_i}$  value of each IMF. Then, three IMF components with the larger calculation values are selected as the major IMF components.

The spectrums of original vibration signals and selected three major modes are shown in Figures 8–19. Figures 8–11 are the spectrums of the fault vibration signal of the inner race. Figures 12–15 are the spectrums of the fault vibration signal of the outer race. Figures 16–19 are the spectrums of the fault vibration signal of the rolling element.

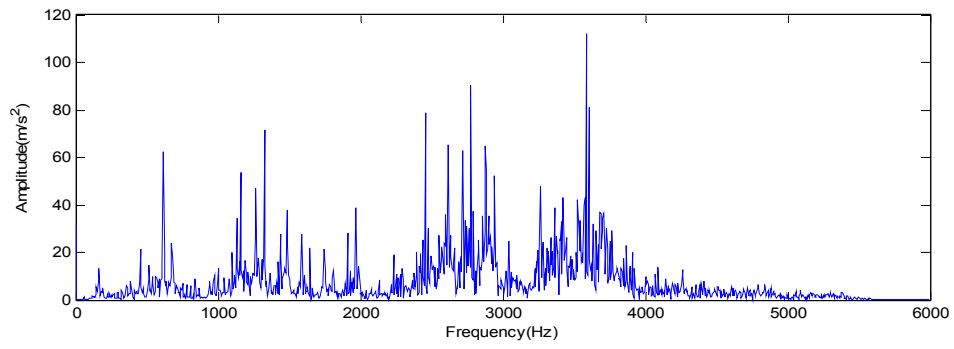


Figure 8. The spectrum of the fault vibration signal of the inner race.

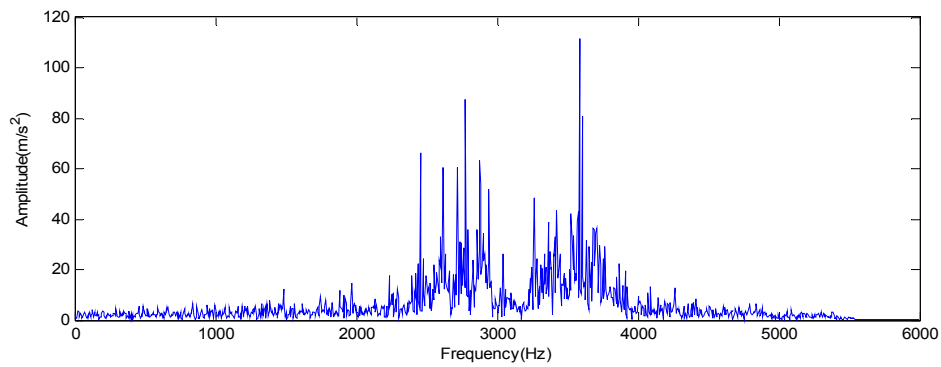


Figure 9. The spectrum of optimal mode of the fault vibration signal of the inner race.

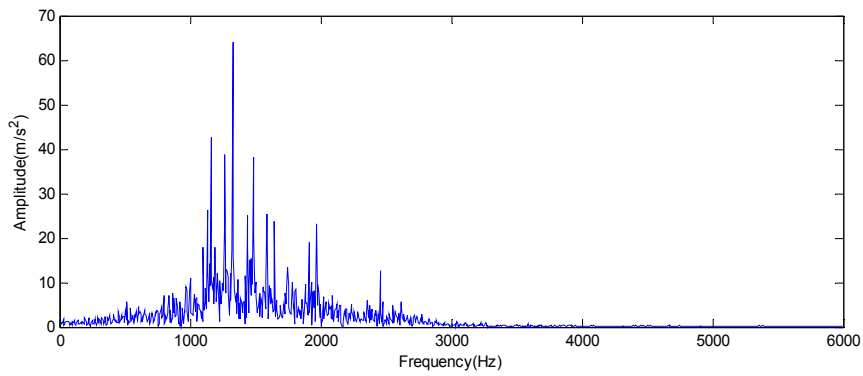


Figure 10. The spectrum of suboptimal mode of the fault vibration signal of the inner race.

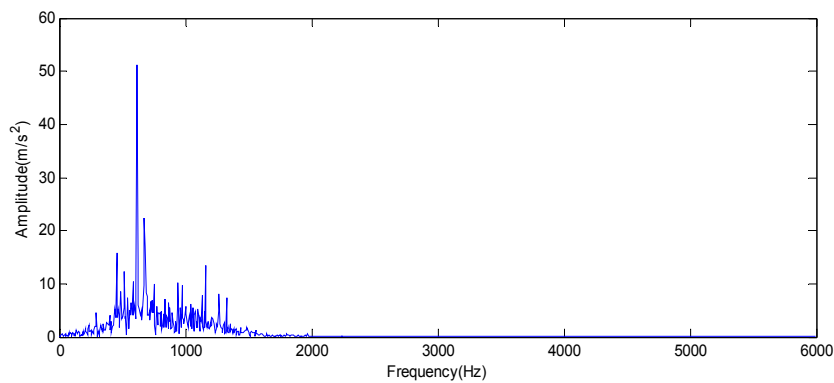


Figure 11. The spectrum of third-optimal mode of the fault vibration signal of the inner race.

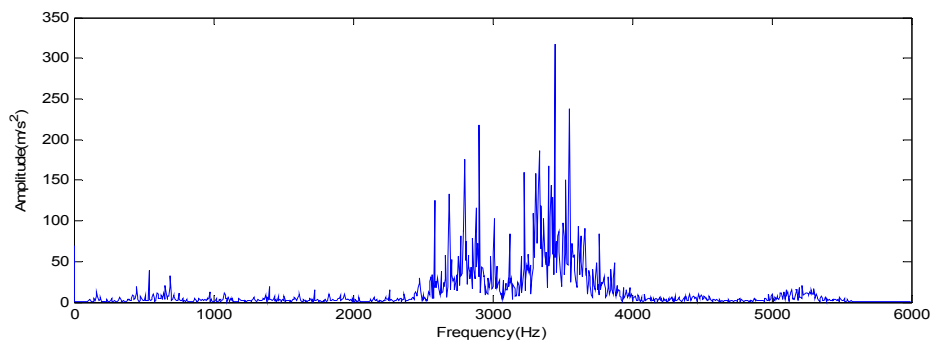


Figure 12. The spectrum of the fault vibration signal of the outer race.

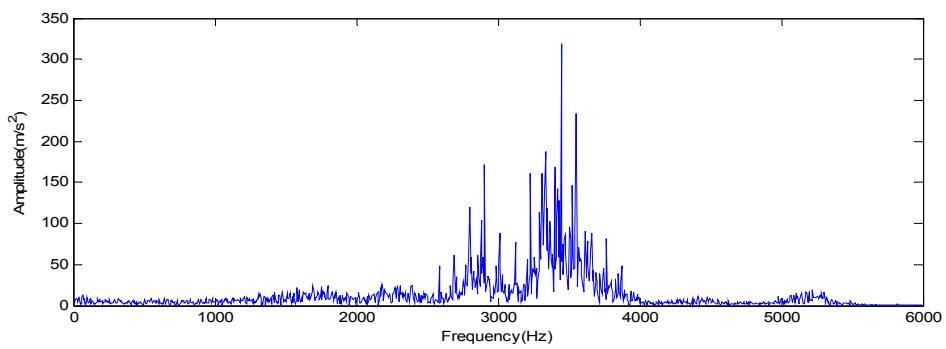


Figure 13. The spectrum of optimal mode of the fault vibration signal of the outer race.

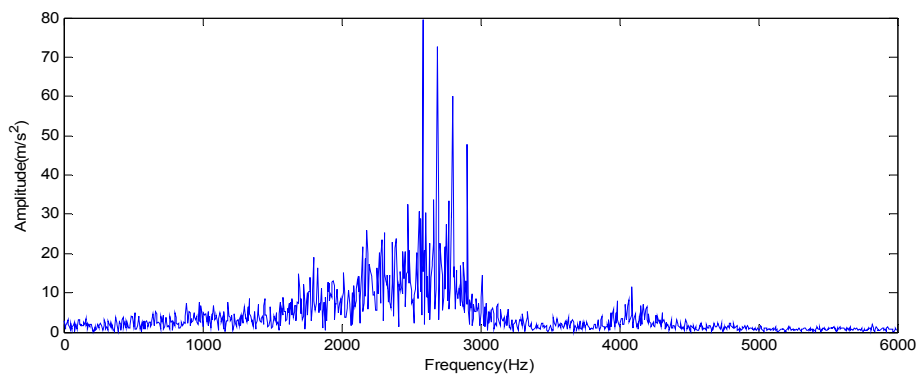


Figure 14. The spectrum of suboptimal mode of the fault vibration signal of the outer race.

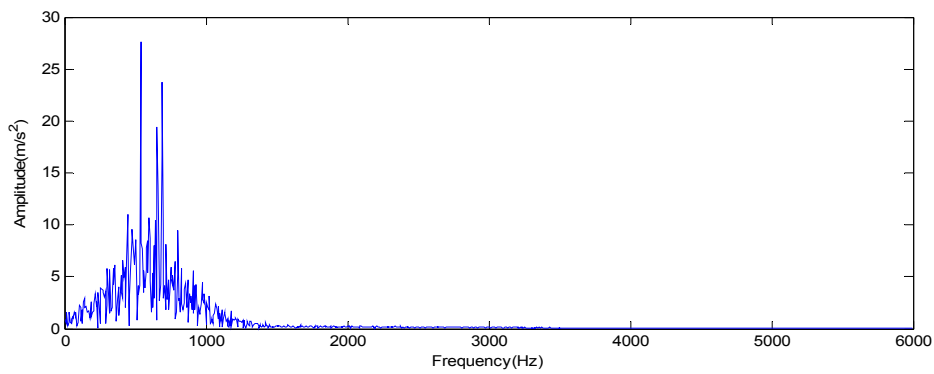
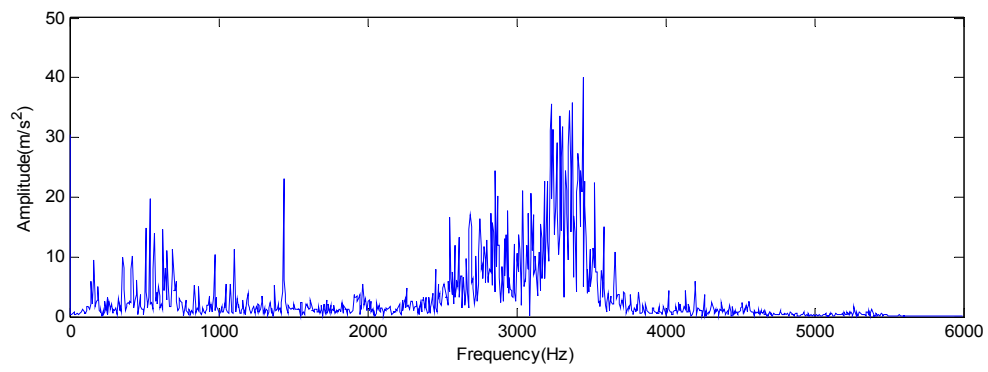
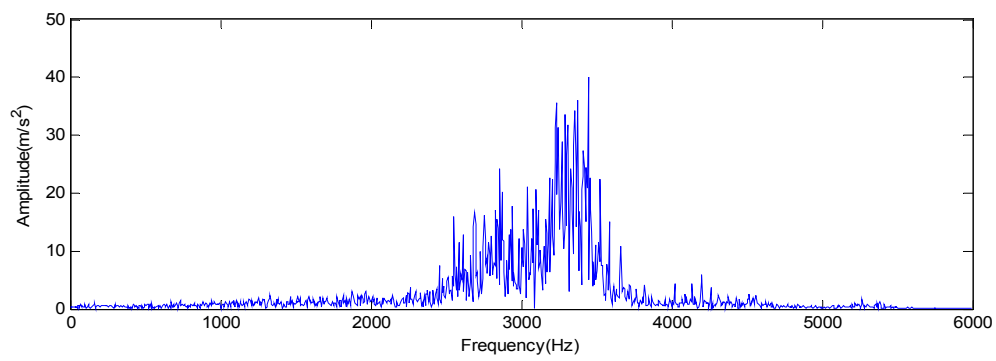


Figure 15. The spectrum of third-optimal mode of the fault vibration signal of the outer race.



**Figure 16.** The spectrum of the fault vibration signal of the rolling element.



**Figure 17.** The spectrum of optimal mode of the fault vibration signal of the rolling element.

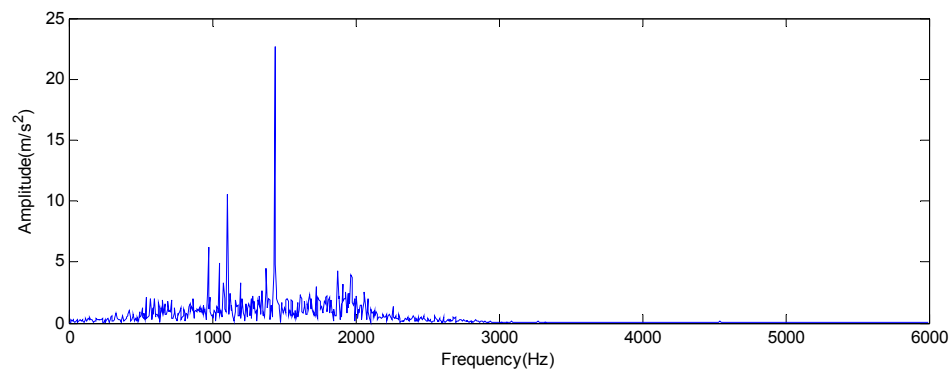


**Figure 18.** The spectrum of suboptimal mode of the fault vibration signal of the rolling element.

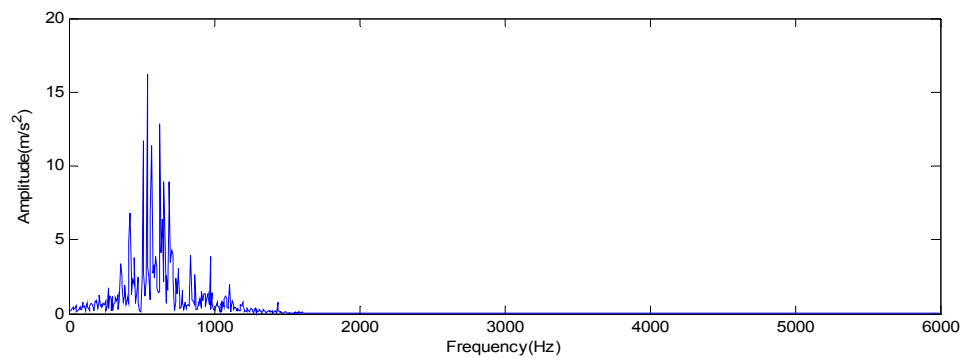


**Figure 19.** The spectrum of three-optimal mode of the fault vibration signal of the rolling element.

#### 4.4. Feature Extraction Based on Multi-Scale Fuzzy Entropy

According to the definition of multi-scale fuzzy entropy, four parameters—embedded dimension  $m$ , the scale factor  $\tau$ , similar tolerance  $r$ , and gradient of fuzzy function  $n$ —must be fixed for each calculation.

In the previous experiments, the alternative values were tested and modified for some feature exaction case in order to obtain the most reasonable initial values of these parameters. Moreover, according to the references regarding parameter selection, these selected values of the parameters take on an improved effect of feature exaction. The embedded dimension is  $m = 0.2$ , the scale factor is  $\tau = 1, 2, 3, 4, 5$ , similar tolerance is  $r = 0.15 SD$ , and the gradient of fuzzy function is  $n = 2$  in this paper.

The values of the multi-scale fuzzy entropy of the three selected major modes are calculated under the scale factor  $\tau = 1, 2, 3, 4, 5$ . Each feature vector obtains 15 entropy values.

The motor bearing with no-load and a fault diameter of 0.007 in. is selected here. The values of the multi-scale fuzzy entropy of the different vibration signals are shown in Tables 1–3. The partial values of multi-scale fuzzy entropy are given due to the limited space of paper.

**Table 1.** The entropy values of the major IMFS of the inner race fault.

Major Modes	Optimal Mode					Suboptimal Mode					Three-Optimal Mode					
	$\tau$	1	2	3	4	5	1	2	3	4	5	1	2	3	4	5
Entropy Values	1	1.05	0.79	0.62	0.41	0.45	0.83	1.17	1.00	0.90	0.88	0.69	1.05	1.42	1.51	1.43
	2	1.02	0.74	0.65	0.46	0.45	0.85	1.21	1.01	0.88	0.83	0.70	1.09	1.46	1.55	1.52
	⋮	⋮	⋮	⋮	⋮	⋮	⋮	⋮	⋮	⋮	⋮	⋮	⋮	⋮	⋮	⋮
	40	1.06	0.78	0.64	0.43	0.51	0.86	1.18	0.96	0.89	0.80	1.69	1.07	1.42	1.50	1.43

**Table 2.** The entropy values of the major IMFS of the outer race fault.

Major Modes	Optimal Mode					Suboptimal Mode					Three-Optimal Mode					
	$\tau$	1	2	3	4	5	1	2	3	4	5	1	2	3	4	5
Entropy Values	1	0.46	0.43	0.34	0.17	0.29	0.76	0.94	0.68	0.59	0.49	0.01	0.24	0.04	0.05	0.06
	2	0.44	0.43	0.32	0.17	0.29	0.80	1.03	0.76	0.60	0.56	0.00	0.01	0.01	0.02	0.02
	⋮	⋮	⋮	⋮	⋮	⋮	⋮	⋮	⋮	⋮	⋮	⋮	⋮	⋮	⋮	⋮
	40	0.43	0.43	0.30	0.17	0.28	0.74	0.81	0.90	0.71	0.56	0.54	0.00	0.01	0.01	0.02

**Table 3.** The entropy values of the major IMFS of the rolling element fault.

Major Modes	Optimal Mode					Suboptimal Mode					Three-Optimal Mode					
	$\tau$	1	2	3	4	5	1	2	3	4	5	1	2	3	4	5
Entropy Values	1	1.05	0.75	0.84	0.37	0.61	0.64	0.78	1.00	1.23	1.28	0.01	0.01	0.02	0.03	0.04
	2	1.00	1.75	0.79	0.35	0.60	0.63	0.75	0.99	1.21	1.29	0.00	0.01	0.01	0.01	0.01
	⋮	⋮	⋮	⋮	⋮	⋮	⋮	⋮	⋮	⋮	⋮	⋮	⋮	⋮	⋮	⋮
	40	1.05	0.79	0.81	0.41	0.62	0.65	0.81	1.06	1.29	1.47	0.02	0.04	0.07	0.09	0.11

## 5. The Experiment Validation and Result Analysis

### 5.1. Effectiveness Validation and Comparative Analysis of the Proposed Method

The motor bearing with no-load and a fault diameter of 0.007 in. is selected to validate and analyze the effectiveness of the proposed method in this section.

The original data were divided into segments of samples where each sample covered 2048 data points. Each of the three fault states (the inner race fault, the outer race fault, and the rolling element fault) includes 40 samples. There are 60 samples for training and 60 samples for testing. The dataset consists of 120 data samples of three fault states.

The SVM with small sample classification and the short training time is selected as a classifier here. The obtained values of multi-scale fuzzy entropy are selected as characteristic vectors. That is to say,  $T = [MFE1, MFE2, MFE3, \dots, MFE15]$  is selected to form characteristic vectors. Then, the characteristic

vectors  $T$  is input into the SVM model to train the SVM model and obtain the SVM classifier. The diagnosis results of the testing samples are shown in Table 4.

**Table 4.** The diagnosis results of test samples.

States	Test Samples	Correctness Diagnosis	Correctness Rate (%)
Inner race fault	20	20	100
Outer race fault	20	20	100
Rolling element fault	20	20	100

In order to verify the effectiveness of the proposed EOMSMFD method for feature extraction and fault diagnosis, the EDOFSFD method based on EEMD, mode selection, and fuzzy entropy is selected here. In the EDOFSFD method, the fuzzy entropy is used to replace multi-scale fuzzy entropy. Thus, the flow and steps of the EDOFSFD method is quite similar to the proposed EOMSMFD method. The EDOFSFD method is not described due to the limited space. The comparison results for two fault diagnosis methods are shown in Table 5.

**Table 5.** Comparison of the diagnosis results for the two fault diagnosis methods.

States	Test Samples	EDOFSFD Method		EOMSMFD Method	
		Correctness Diagnosis	Correctness (%)	Correctness Diagnosis	Correctness (%)
Inner race fault	20	20	100	20	100
Outer race fault	20	20	100	20	100
Rolling element fault	20	5	25	20	100

As can be seen from Table 5 and Figure 20, for the fault vibration signal of the inner race and the outer race, it can be seen that the proposed EDOFSFD method and the EOMSMFD method can both obtain a diagnosis accuracy of 100%. However, for the fault vibration signal of the rolling element, it can be seen that the test accuracy of the proposed EOMSMFD method and the EDOFSFD method is 100% and 25% in the experiments, respectively. Thus, the proposed EOMSMFD method has a higher diagnosis accuracy than the EDOFSFD method. For the EDOFSFD method and the EOMSMFD method, the EEMD, mode selection, and SVM are the same. Multi-scale fuzzy entropy is used to extract the feature from the vibration signal in the proposed EOMSMFD method, and fuzzy entropy is used to extract the feature from the vibration signal in the proposed EDOFSFD method. This shows that the multi-scale fuzzy entropy can better extract features from the vibration signal than can fuzzy entropy. Thus, the feature extraction and fault diagnosis capabilities of the proposed EOMSMFD method outperform the EDOFSFD method. The EOMSMFD method is the most effective method for extracting the fault feature from the collected vibration signal and for diagnosing the faults.



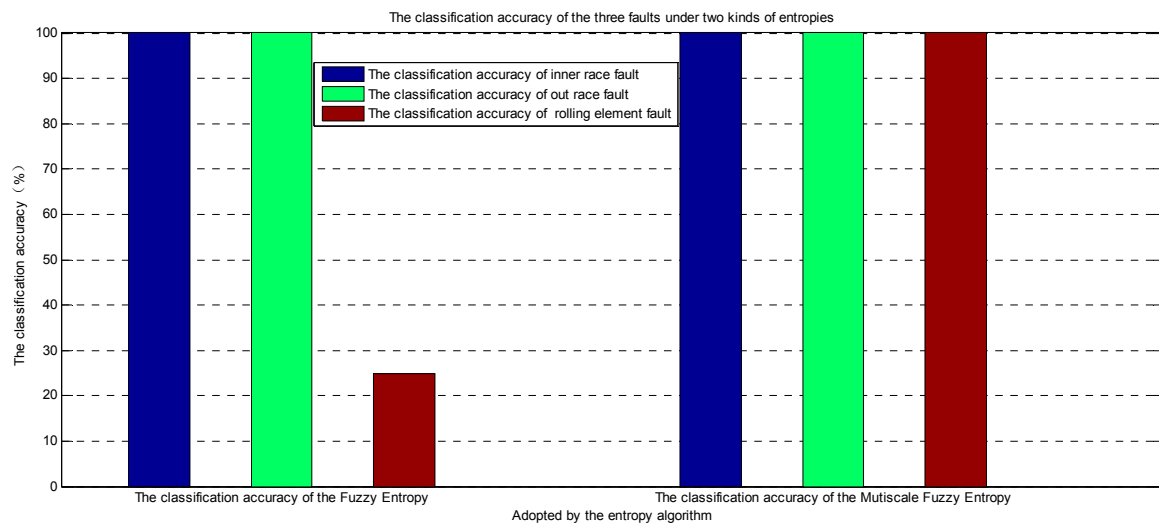


Figure 20. The classification accuracy of the three faults for the two fault diagnosis methods.

5.2. Diagnosis Results and Analysis under Different Loads

In order to verify the effectiveness of the proposed EOMSMFD method under load changes, the fault feature extraction and classification of the inner race fault, the outer race fault, and the rolling element fault of the motor bearing under no-load and 3HP loads are studied and analyzed. Fault diameters of 0.007 and 0.021 in. are selected here.

The original data were divided into segments of samples where each sample covered 2048 data points. For each fault under each fault severity and each load, there were 40 samples. Twenty samples were randomly selected as training samples, and the remaining 20 samples were selected as testing samples. Four hundred eighty samples for the motor bearing were obtained here. For each fault diameter, hybrid samples of no-load and 3HP loads were used to diagnose fault type. The diagnosis results are shown in Table 6.

Table 6. The diagnosis results of the test samples under 3HP loads and no-load.

States	No-Load and 3HP Loads			
	0.007 in.		0.021 in.	
	Test Samples	Correctness Rate (%)	Test Samples	Correctness Rate (%)
Inner race fault	40	100	40	100
Outer race fault	40	100	40	100
Rolling element fault	40	100	40	100

As can be seen from Table 6, for the inner race, the outer race, and the rolling element of the motor bearing, the correctness rates of fault diagnosis are 100% for the motors under no-load and the 3HP load and the fault diameters for 0.007 and 0.021 in., respectively. The experiment results show that the proposed method does not have any influence and is very stable for different loads. That is, the proposed method is not sensitive to the load on the motor. It takes on an improved stability and effectiveness in fault diagnosis for the motor under different loads.

5.3. Diagnosis Results and Analysis under Different Fault Severities

In order to verify the effectiveness of the proposed EOMSMFD method for different fault severities, the fault types and fault severities of the inner race, the outer race, and the rolling element of the motor bearing are diagnosed. The motor with fault diameters of 0.007 and 0.021 in. under 3HP load is selected here.

The original data were divided into segments of samples where each sample covered 2048 data points. For each fault type under each fault severity, there were 40 samples. Twenty samples were randomly selected as training samples, and the remaining 20 samples were selected as testing samples. Four hundred eighty samples for the motor bearing were obtained here. The hybrid samples of fault diameters of 0.007 and 0.021 in. were used to diagnose fault type and fault severity. The diagnosis results are shown in Table 7.

**Table 7.** Comparison of the diagnosis results of the test samples.

Results	Inner Race Fault		Outer Race Fault		Rolling Element Fault	
	0.007 in.	0.021 in.	0.007 in.	0.021 in.	0.007 in.	0.021 in.
Correctness rate for classification	100	100	100	100	100	100
Correctness rate for fault severity	100	100	100	100	95	100

As can be seen from Table 7, for the inner race and the outer race faults of the motors with 3HP loads and fault diameters of 0.007 and 0.021 in., the correctness rate of classification and the correctness rate of fault severity are 100%, respectively. For the rolling element fault of the motors with 3HP loads and fault diameters of 0.021 in., the correctness rate of classification and the correctness rate of fault severity are both 100%. However, for the rolling element fault of the motors with 3HP loads and fault diameters of 0.007 in., the correctness rate of classification are 95%, and the correctness rate of fault severity is 100%. The experiment results show that the proposed method does not have any influence and is effective for different fault severities on the motor bearing. That is, the proposed method can effectively diagnose the fault for different severities on the motor bearing. Thus, the proposed method is an effective method for realizing the fault types and fault severities of the inner race, the outer race, and the rolling element of the motor bearing.

To summarize, the proposed EOMSMFD method mainly has the following advantages:

(1) The EEMD can effectively decompose the vibration signal into a series of IMFs and residual components. Moreover, it can effectively avoid the mode mixing phenomenon.

(2) The correlation coefficient method can effectively select three corresponding sensitive IMFs to represent the original signal. It can not only extract the effective mode and reduce the workload, but can also avoid dealing with useless modes.

(3) Multi-scale fuzzy entropy can better extract fault features from the vibration signals than can fuzzy entropy. The extracted fault features take on an improved distinguishing ability.

(4) The proposed EOMSMFD method is an effective fault diagnosis method for motor bearings. Moreover, this method does not have any influence on motors with different loads and different fault severities. It can effectively diagnose fault types and fault severities on motor bearings. Moreover, it takes on an improved stability and effectiveness in fault diagnosis for motors under different loads and different fault severities.

## 6. Conclusions

To perfectly extract the multiple scale characteristics of the vibration signal of the motor bearing and well diagnose its faults, a novel feature extraction (EDOMFE) method is proposed in this paper. The proposed method integrates EEMD, mode selection, and multi-scale fuzzy entropy. Moreover, the SVM is used as a classifier to obtain a fault diagnosis (EOMSMFD) method. The EEMD method is used to decompose the nonlinear and non-stationary vibration signals of the inner ring, the outer ring, and the rolling element of the motor bearing, and the IMFs with small modal mixing are obtained. The correlation coefficient analysis method is used to calculate and determine three improved IMFs, which are close to the original signal. Then, the multi-scale fuzzy entropy is used to calculate the entropy values for the three selected IMFs in order to generate the fault feature vector, which is input into SVM classifier to identify the fault types and fault severities. The effectiveness of the proposed

method is fully evaluated by experiments and comparative studies. The experiment results show that the proposed method provides an improved recognition performance under the motor with different loads and different fault severities. The recognition rates of the inner race, the outer race, and the rolling element of the motor bearing, with hybrid samples of no-load and 3HP loads, reach 100% under the fault diameters of 0.007 or 0.021 in., respectively. For the motors with hybrid samples of fault diameters of 0.007 and 0.021 in. under 3HP loads, the recognition rate of classification and the recognition rate of fault severity are 100% for the inner race and the outer race of the motor bearing, and the recognition rate of classification is 95% and the recognition rate of fault severity is 100% for the rolling element of the motor bearing. Moreover, the comparative studies with the other mentioned methods show that the multi-scale fuzzy entropy can extract much more diagnostic information compared with fuzzy entropy, and the proposed method can effectively eliminate the influence of the mode mixing. Thus, the proposed method is found to be an effective method for the fault diagnosis of the motor bearing and has potential application for other rotating machinery.

Due to the lower computational efficiency of the proposed method, in future work, we will attempt to improve the computational efficiency for obtaining the fault feature vector by using multi-scale fuzzy entropy. The goal is to develop a real-time fault diagnosis system for rotating machinery.

**Acknowledgments:** The authors would like to thank all the reviewers for their constructive comments. This research was supported by the National Natural Science Foundation of China (51605068, 51475065, U1433124), the Open Project Program of State Key Laboratory of Mechanical Transmissions (Chongqing University) (SKLMT-KFKT-201513, SKLMT-KFKT-201416), the Open Project Program of the Traction Power State Key Laboratory of Southwest Jiaotong University (TPL1705, TPL1403), the Science and Technology Project of Liaoning Provincial Department of Education (JDL2016030), the Doctoral Scientific Research Foundation of Liaoning Province (201601264), the Natural Science Foundation of Liaoning Province (2015020013, 201602140), and the Open Project Program of Sichuan Provincial Key Lab of Process Equipment and Control (GK201613). The program for the initialization, study, training, and simulation of the proposed algorithm in this article was written with the tool-box of MATLAB 2010b produced by the Math-Works, Inc.

**Author Contributions:** Huimin Zhao conceived the research subject and contributed to feature extraction, Meng Sun contributed to mode selection, Wu Deng contributed to multi-scale fuzzy entropy, and Xinhua Yang carried out the experiments. All authors have read and approved the final manuscript.

**Conflicts of Interest:** The authors declare no conflict of interest.

## References

1. Yang, Z.X.; Zhong, J.H. A hybrid EEMD-based sampEn and SVD for acoustic signal processing and fault diagnosis. *Entropy* **2016**, *18*, 112. [[CrossRef](#)]
2. Gu, B.; Sheng, V.S.; Wang, Z.J.; Ho, D.; Osman, S.; Li, S. Incremental learning for  $\nu$ -Support Vector Regression. *Neural Netw.* **2015**, *67*, 140–150. [[CrossRef](#)] [[PubMed](#)]
3. Xia, Z.H.; Wang, X.H.; Sun, X.M.; Wang, B.W. Steganalysis of least significant bit matching using multi-order differences. *Secur. Commun. Netw.* **2014**, *7*, 1283–1291. [[CrossRef](#)]
4. Rubini, R.; Meneghetti, U. Application of the envelope and wavelet transform analyses for the diagnosis of incipient faults in ball bearings. *Mech. Syst. Signal Process.* **2001**, *15*, 287–302. [[CrossRef](#)]
5. Zheng, Y.H.; Jeon, B.; Xu, D.H.; Wu, Q.M.J.; Zhang, H. Image segmentation by generalized hierarchical fuzzy C-means algorithm. *J. Intell. Fuzzy Syst.* **2015**, *28*, 961–973.
6. Seker, S.; Ayaz, E. Feature extraction related to bearing damage in electric motors by wavelet analysis. *J. Frankl. Inst.* **2003**, *340*, 125–134. [[CrossRef](#)]
7. Yang, Y.; Yu, D.J.; Cheng, J.S. A roller bearing fault diagnosis method based on EMD energy entropy and ANN. *J. Sound Vib.* **2006**, *294*, 269–277.
8. Cheng, J.S.; Yu, D.J.; Yang, Y. A fault diagnosis approach for roller bearings based on EMD method and AR model. *Mech. Syst. Signal Process.* **2006**, *20*, 350–362.
9. Cheng, J.S.; Yu, D.J.; Tang, J.S.; Yang, Y. Local rub-impact fault diagnosis of the rotor systems based on EMD. *Mech. Mach. Theory* **2009**, *44*, 784–791. [[CrossRef](#)]
10. Immovilli, F.; Bellini, A.; Rubini, R.; Tassoni, C. Diagnosis of bearing faults in induction machines by vibration or current signals: A critical comparison. *IEEE Trans. Ind. Appl.* **2010**, *46*, 1350–1359. [[CrossRef](#)]

11. Lei, Y.G.; He, Z.J.; Zi, Y.Y. EEMD method and WNN for fault diagnosis of locomotive roller bearings. *Expert Syst. Appl.* **2011**, *38*, 7334–7341. [[CrossRef](#)]
12. Wang, D.; Guo, W.; Wang, X.J. A joint sparse wavelet coefficient extraction and adaptive noise reduction method in recovery of weak bearing fault features from a multi-component signal mixture. *Appl. Soft Comput. J.* **2013**, *13*, 4097–4104. [[CrossRef](#)]
13. Liu, T.; Chen, J.; Dong, G.M.; Xiao, W.B.; Zhou, X.N. The fault detection and diagnosis in rolling element bearings using frequency band entropy. *J. Mech. Eng. Sci.* **2013**, *227*, 87–99. [[CrossRef](#)]
14. Wang, Z.P.; Lu, C.; Wang, Z.L.; Liu, H.M.; Fan, H.Z. Fault diagnosis and health assessment for bearings using the Mahalanobis-Taguchi system based on EMD-SVD. *Trans. Inst. Meas. Control* **2013**, *35*, 798–807. [[CrossRef](#)]
15. Liao, Q.; Li, X.B.; Huang, B. Hybrid fault-feature extraction of rolling element bearing via customized-lifting multi-wavelet packet transform. *J. Mech. Eng. Sci.* **2014**, *228*, 2204–2216. [[CrossRef](#)]
16. Wang, H.C.; Chen, J.; Dong, G.M. Feature extraction of rolling bearing's early weak fault based on EEMD and tunable Q-factor wavelet transform. *Mech. Syst. Signal Process.* **2014**, *48*, 103–119. [[CrossRef](#)]
17. Ahn, J.H.; Kwak, D.H.; Koh, B.H. Fault detection of a roller-bearing system through the EMD of a wavelet denoised signal. *Sensors* **2014**, *14*, 15022–15038. [[CrossRef](#)] [[PubMed](#)]
18. Jiang, F.; Zhu, Z.C.; Li, W.; Chen, G.A.; Zhou, G.B. Robust condition monitoring and fault diagnosis of rolling element bearings using improved EEMD and statistical features. *Meas. Sci. Technol.* **2014**, *25*, 025003. [[CrossRef](#)]
19. Zhu, K.H.; Song, X.G.; Xue, D.X. A roller bearing fault diagnosis method based on hierarchical entropy and support vector machine with particle swarm optimization algorithm. *Measurement* **2014**, *47*, 669–675. [[CrossRef](#)]
20. Gao, H.Z.; Liang, L.; Chen, X.G.; Xu, G.H. Feature extraction and recognition for rolling element bearing fault utilizing short-time fourier transform and non-negative matrix factorization. *Chin. J. Mech. Eng.* **2015**, *28*, 96–105. [[CrossRef](#)]
21. Henao, H.; Capolino, G.A.; Manes, F.C.; Filippetti, F.; Bruzzese, C.; Strangas, E.; Pusca, R.; Estima, J.; Martin, R.G.; Shahin, H.K. Trends in fault diagnosis for electrical machines: A review of diagnostic techniques. *IEEE Ind. Electron. Mag.* **2014**, *8*, 31–42. [[CrossRef](#)]
22. Lucia, F.; Ciprian, H.; Lorand, S. Induction machine bearing fault detection by means of statistical processing of the stray flux measurement. *IEEE Trans. Ind. Electron.* **2015**, *62*, 1846–1854.
23. Wang, D.; Sun, S.L.; Tse, P.W. A general sequential Monte Carlo method based optimal wavelet filter: A Bayesian approach for extracting bearing fault features. *Mech. Syst. Signal Process.* **2015**, *52–53*, 293–308. [[CrossRef](#)]
24. He, W.P.; Zi, Y.Y.; Chen, B.Q.; Wu, F.; He, Z.J. Automatic fault feature extraction of mechanical anomaly on induction motor bearing using ensemble super-wavelet transform. *Mech. Syst. Signal Process.* **2015**, *54*, 457–480. [[CrossRef](#)]
25. Wang, H.C.; Chen, J.; Dong, G.M. Fault diagnosis of rolling bearing's early weak fault based on minimum entropy de-convolution and fast Kurtogram algorithm. *J. Mech. Eng. Sci.* **2015**, *229*, 2890–2907. [[CrossRef](#)]
26. Wang, C.; Gan, M.; Zhu, C.A. Non-negative EMD manifold for feature extraction in machinery fault diagnosis. *Measurement* **2015**, *70*, 188–202. [[CrossRef](#)]
27. Shi, P.M.; An, S.J.; Li, P.; Han, D.Y. Signal feature extraction based on cascaded multi-stable stochastic resonance denoising and EMD method. *Measurement* **2016**, *90*, 318–328. [[CrossRef](#)]
28. Wang, Y.; Liu, D.; Xu, G.H.; Jian, K.S. An image dimensionality reduction method for rolling bearing fault diagnosis based on singular value decomposition. *J. Mech. Eng. Sci.* **2016**, *230*, 1830–1845. [[CrossRef](#)]
29. Li, Y.B.; Xu, M.Q.; Wei, Y.; Huang, W.H. A new rolling bearing fault diagnosis method based on multiscale permutation entropy and improved support vector machine based binary tree. *Measurement* **2016**, *77*, 80–94. [[CrossRef](#)]
30. Pincus, S.M. Approximate entropy as a measure of system complexity. *Proc. Natl. Acad. Sci. USA* **1991**, *88*, 2297–2301. [[CrossRef](#)] [[PubMed](#)]
31. Zhao, S.F.; Liang, L.; Xu, G.H.; Wang, J.; Zhang, W.M. Quantitative diagnosis of a spall-like fault of a rolling element bearing by empirical mode decomposition and the approximate entropy method. *Mech. Syst. Signal Process.* **2013**, *40*, 154–177. [[CrossRef](#)]
32. Richman, J.S.; Moorman, J.R. Physiological time series analysis using approximate entropy and sample entropy. *Am. J. Physiol. Heart Circ. Physiol.* **2000**, *278*, 2039–2049.

33. Chen, W.; Wang, Z.; Xie, H.; Yu, W. Characterization of surface EMG signal based on fuzzy entropy. *IEEE Trans. Neural Syst. Rehabil. Eng.* **2007**, *15*, 266–272. [[CrossRef](#)] [[PubMed](#)]
34. Chen, W.T.; Zhuang, J.; Yu, W.X.; Wang, Z. Measuring complexity using FuzzyEn, ApEn and SampEn. *Med. Eng. Phys.* **2009**, *31*, 61–68. [[CrossRef](#)] [[PubMed](#)]
35. Dong, S.J.; Tang, B.P.; Chen, R.X. Bearing running state recognition based on non-extensive wavelet feature scale entropy and support vector machine. *Measurement* **2013**, *46*, 4189–4199. [[CrossRef](#)]
36. Zhang, L.; Xiong, G.L.; Liu, H.S.; Zou, H.J.; Guo, W.Z. Bearing fault diagnosis using multi-scale entropy and adaptive neuro-fuzzy inference. *Expert Syst. Appl.* **2010**, *37*, 6077–6085. [[CrossRef](#)]
37. Liu, H.H.; Han, M.H. A fault diagnosis method based on local mean decomposition and multi-scale entropy for roller bearings. *Mech. Mach. Theory* **2014**, *75*, 67–78. [[CrossRef](#)]
38. Vakharia, V.; Gupta, V.K.; Kankar, P.K. A multiscale permutation entropy based approach to select wavelet for fault diagnosis of ball bearings. *J. Vib. Control* **2015**, *21*, 3123–3131. [[CrossRef](#)]
39. Tiwari, R.; Gupta, V.K.; Kankar, P.K. Bearing fault diagnosis based on multi-scale permutation entropy and adaptive neuro fuzzy classifier. *J. Vib. Control* **2015**, *21*, 461–467. [[CrossRef](#)]
40. Chen, X.; Jin, N.D.; Zhao, A.; Gao, Z.K.; Zhai, L.S.; Sun, B. The experimental signals analysis for bubbly oil-in-water flow using multi-scale weighted-permutation entropy. *Physica A* **2015**, *417*, 230–244. [[CrossRef](#)]
41. Zheng, J.D.; Cheng, J.S.; Yang, Y.; Luo, S.R. A rolling bearing fault diagnosis method based on multi-scale fuzzy entropy and variable predictive model-based class discrimination. *Mech. Mach. Theory* **2014**, *78*, 187–200. [[CrossRef](#)]
42. Costa, M.; Goldberger, A.L.; Peng, C.K. Multiscale entropy analysis of complex physiological time series. *Phys. Rev. Lett.* **2002**, *89*, 068102. [[CrossRef](#)] [[PubMed](#)]
43. Wen, X.Z.; Shao, L.; Xue, Y.; Fang, W. A rapid learning algorithm for vehicle classification. *Inf. Sci.* **2015**, *295*, 395–406. [[CrossRef](#)]
44. Gu, B.; Sheng, V.S.; Tay, K.Y.; Romano, W.; Li, S. Incremental Support Vector Learning for Ordinal Regression. *IEEE Trans. Neural Netw. Learn. Syst.* **2015**, *26*, 1403–1416. [[CrossRef](#)] [[PubMed](#)]
45. Gu, B.; Sun, X.M.; Sheng, V.S. Structural Minimax Probability Machine. *IEEE Trans. Neural Netw. Learn. Syst.* **2016**, *PP*, 1–11. [[CrossRef](#)] [[PubMed](#)]
46. Chen, Y.D.; Hao, C.Y.; Wu, W.; Wu, E.H. Robust dense reconstruction by range merging based on confidence estimation. *Sci. China Inf. Sci.* **2016**, *59*, 092103. [[CrossRef](#)]
47. Gu, B.; Sheng, V.S.; Li, S. Bi-parameter space partition for cost-sensitive SVM. In Proceedings of the 24th International Joint Conference on Artificial Intelligence, Buenos Aires, Argentina, 25–31 July 2015; pp. 3532–3539.
48. Kuo, Y.C.; Hsieh, C.T.; Yau, H.T.; Li, Y.C. Research and Development of a Chaotic Signal Synchronization Error Dynamics-Based Ball Bearing Fault Diagnostosr. *Entropy* **2014**, *16*, 5358–5376. [[CrossRef](#)]
49. Wu, S.D.; Wu, C.W.; Wu, T.Y.; Wang, C.C. Multi-scale analysis based ball bearing defect diagnostics using mahalanobis distance and support vector machine. *Entropy* **2013**, *15*, 416–433. [[CrossRef](#)]
50. Bearing Data Center. Available online: <http://csegroups.case.edu/bearingdatacenter/home> (accessed on 27 December 2016).



© 2016 by the authors; licensee MDPI, Basel, Switzerland. This article is an open access article distributed under the terms and conditions of the Creative Commons Attribution (CC-BY) license (<http://creativecommons.org/licenses/by/4.0/>).